

## Inclusive Electron Production in $e^+e^-$ Annihilation at 29 GeV

M. E. Nelson, A. Blondel,<sup>(a)</sup> G. H. Trilling, G. S. Abrams, D. Amidei, C. A. Blocker,  
 A. M. Boyarski, M. Breidenbach, D. L. Burke, W. Chinowsky, W. E. Dieterle,<sup>(b)</sup>  
 J. B. Dillon, J. M. Dorfan, M. W. Eaton, G. J. Feldman, M. E. B. Franklin,  
 G. Gidal, L. Gladney, M. S. Gold, G. Goldhaber, L. J. Golding, G. Hanson,  
 R. J. Hollebeek, W. R. Innes, J. A. Jaros, A. D. Johnson, J. A. Kadyk,  
 A. J. Lankford, R. R. Larsen, B. LeClaire, M. Levi, N. Lockyer,  
 V. Lüth, C. Matteuzzi, J. F. Patrick,<sup>(c)</sup> M. L. Perl, B. Richter,  
 P. C. Rowson, T. Schaad, H. M. Schellman, D. Schlatter,  
 R. F. Schwitters, P. D. Sheldon, J. Strait,<sup>(d)</sup>  
 C. de la Vaissière, J. M. Yelton,  
 and C. Zaiser

*Lawrence Berkeley Laboratory and Department of Physics, University of California, Berkeley,  
 California 94720, and Stanford Linear Accelerator Center, Stanford University,  
 Stanford, California 94305, and Department of Physics, Harvard University,  
 Cambridge, Massachusetts 02138*

(Received 4 March 1983)

The total momentum and transverse momentum spectra of electrons in  $e^+e^-$  annihilation at 29 GeV have been measured. The inclusive cross section is determined to be  $14.4 \pm 1.6 \pm 5.2$  pb for momenta greater than 2 GeV/c. The average semielectronic branching ratios of charm and bottom quarks are measured to be  $(6.3 \pm 1.2 \pm 2.1)\%$  and  $(11.6 \pm 2.1 \pm 1.7)\%$ , respectively. The fragmentation function for bottom quarks is determined to be peaked at high  $z$ , with  $\langle z \rangle_b = 0.75 \pm 0.05 \pm 0.04$ .

PACS numbers: 13.65.+i, 14.80.Dg

Prompt lepton production in hadronic events from high-energy  $e^+e^-$  annihilation is an excellent signal for the presence of hadrons containing charm ( $c$ ) or bottom ( $b$ ) quarks. The production rates and momentum spectra of such leptons depend on the weak-decay semileptonic branching ratios and the momentum spectra of the parent hadrons. In turn the momentum spectra of these hadrons provide information on the fragmentation properties of  $c$  and  $b$  quarks. Simple kinematical considerations suggest that, as quark masses increase, hadrons containing the heavy quark carry an increasing fraction of its momentum.<sup>1</sup> This situation contrasts with the observation that light quarks fragment principally into low-momentum hadrons. There is recent experimental evidence that charm-quark fragmentation does lead to a harder momentum spectrum than is the case for light-quark fragmentation.<sup>2-4</sup> In this Letter we obtain the first experimental information on  $b$ -quark fragmentation.

In this analysis we measure the total momentum and transverse momentum spectra of prompt electrons in hadronic events from  $e^+e^-$  annihilation at a center of mass (c.m.) energy of 29 GeV. The transverse momentum  $p_\perp$  is measured with respect to the thrust axis defined by all the

charged particles in the event. The harder  $p_\perp$  distribution of electrons from bottom decays relative to charm decays allows us to separate the contributions of  $b$  and  $c$  quarks to the prompt electron signal.<sup>5</sup>

The data, collected with the MARK II detector at the electron-positron storage ring PEP at the Stanford Linear Accelerator Center, correspond to an integrated luminosity of  $35 \text{ pb}^{-1}$ . The MARK II detector has been described elsewhere,<sup>6</sup> and we recall here only the elements essential to our analysis. Charged-particle momenta are measured over 76% of  $4\pi$  in a cylindrical drift chamber in an axial magnetic field. The rms momentum resolution is given by  $(\delta p/p)^2 \simeq (0.015)^2 + (0.01 p)^2$ , where the momentum  $p$  is in units of GeV/c. Electron identification is accomplished over 64% of  $4\pi$  by combining this momentum determination with measurements of energy deposition in a lead-liquid-argon calorimeter.<sup>7</sup> In this calorimeter, spatial information is obtained by sampling energy depositions on strips which run in three different directions.

The electron-hadron separation algorithm is based on measurements of the ratio  $r_i \equiv E_i/p$ , where  $E_i$  is the energy deposition in one of three groupings,  $i = 1-3$ , of layers in the calorimeter.

Each of these groupings combines all layers in the first 8 radiation lengths which have the same strip orientation. To minimize the effects of neighboring particles, particularly photons, the energy deposition  $E_i$  is taken from a narrow lateral region, comparable in size to a strip width ( $\approx 4$  cm), centered about the extrapolated particle trajectory. The algorithm demands that *each* value of  $r_i$  and that  $\sum r_i$  be greater than an appropriate minimum value. The electron identification efficiency was determined with electrons from Bhabha events and photon conversions. This efficiency varies from 78% at 1 GeV/c to 93% at the highest momenta.

We determined the probability, as a function of  $p$  and  $p_\perp$ , that a hadron will be misidentified as an electron as follows. First, hadron interactions in our calorimeter were studied with use of data taken in a pion beam and with use of pions from the decay  $\psi \rightarrow 2(\pi^+\pi^-)\pi^0$  in data taken at the SPEAR storage ring. Second, to measure the effect of accidental overlap with nearby photons, we took advantage of the back-to-back jet topology of most hadronic events at 29 GeV. Charged tracks in these events were reversed and projected to the opposite jet. Energy depositions associated with the inverted track arise purely from accidental overlap. To determine overall misidentification probabilities we added hadron energy depositions, obtained from the beam test and  $\psi$  data, to the overlap contributions, and input the sums into the electron-hadron separation algorithm. The misidentification probabilities are typically 0.5%, but can be as large as 3% for a track of momentum 1 GeV/c in the core of a jet.

A hadronic event sample was selected by requiring a charged multiplicity of at least five and total detected energy (charged plus neutral) greater than 25% of the c.m. energy. There were a total of 10 691 such events. In this sample there are sources of real electrons which are not part of the prompt signal. A visual scan was performed to remove a small number of electron candidates arising from  $\tau$  pair production, beam-gas interactions, and the process  $e^+e^- \rightarrow e^+e^- + \text{hadrons}$ . Background electrons from photon conversions and Dalitz decays were removed by a pair-finding algorithm, which searched for low-invariant-mass combinations with oppositely charged tracks. This algorithm removes about 70% of the electrons coming from pairs while only removing 2% of the real prompt electrons. After removal of these backgrounds on

an event by event basis, 930 electron candidates with  $p > 1$  GeV/c remained. These were partitioned into 24  $p, p_\perp$  bins.

In each  $p, p_\perp$  bin, we subtracted the remaining backgrounds and corrected for geometrical and identification efficiencies. The background from misidentified hadrons was calculated from the number of observed charged hadron tracks in each bin and the appropriate misidentification probability. The background from remaining electron pairs was calculated by use of the number of electrons from identified pairs in each bin and the known efficiency of the pair-finding algorithm. Figure 1 shows the corrected signal in all 24 bins. The systematic errors shown are dominated by the uncertainty in the hadron misidentification probabilities. In three of the lowest momentum and transverse momentum bins [Fig. 1(a),  $p < 3.0$  GeV/c and Fig. 1(b),  $p < 2.0$  GeV/c] backgrounds account for almost 75% of the observed signal; thus these points have substantial systematic errors. Excluding these three bins, the background fractions for Figs. 1(a)–1(d) are 46%, 36%, 30%, and 23%, respec-

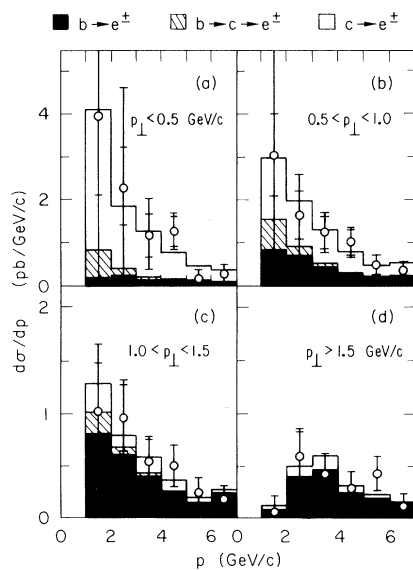


FIG. 1. Prompt-electron momentum spectra in four regions of transverse momentum  $p_\perp$  (GeV/c): (a)  $p_\perp < 0.5$ , (b)  $0.5 < p_\perp < 1.0$ , (c)  $1.0 < p_\perp < 1.5$ , and (d)  $p_\perp > 1.5$ . Two sets of error bars are shown for each data point. The smaller ones are statistical only. The larger ones are the statistical and systematic errors added in quadrature. The highest momentum bin includes all momenta  $\geq 6$  GeV/c. The histograms show the results of the fit. The three contributions shown are (i)  $b$  primary (solid), (ii)  $c$  secondary (diagonally hatched), and (iii)  $c$  primary (unshaded).

tively. Figure 2 shows the total momentum and transverse momentum differential cross sections for prompt electrons with  $p > 2$  GeV/c. The total inclusive cross section for this momentum range is determined to be  $14.4 \pm 1.6 \pm 5.2$  pb.

We have performed a maximum-likelihood fit to the observed populations in the various  $p, p_\perp$  bins, accounting for the signal above background in terms of the following contributions: (i) bottom decays in  $b\bar{b}$  events ( $b$  primary); (ii) charm decays in  $b\bar{b}$  events ( $c$  secondary); and (iii) charm decays in  $c\bar{c}$  events ( $c$  primary). We have excluded from the fit the three bins in which the background contributions strongly dominate. To represent contributions (i)–(iii) we have used a Monte Carlo simulation with a Feynman-Field hadronization model<sup>8</sup> and gluon radiation as incorporated by Ali *et al.*<sup>9</sup> We have verified that the semileptonic electron spectra produced by the heavy-meson decay models in the Monte Carlo simulation agree satisfactorily with measured spectra from the DELCO<sup>10</sup> (charm) and CLEO<sup>11</sup> (bottom) experiments.

We have parametrized the fragmentation function  $D_Q^H$  for quark  $Q$  into hadron  $H$  by an expression of the form<sup>12</sup>

$$D_Q^H(z) = \frac{A}{z[1 - 1/z - \epsilon_Q/(1-z)]^2}, \quad (1)$$

where  $z$  is the ratio of hadron energy to quark energy,  $A$  is a normalization factor, and  $\epsilon_Q$  is a parameter. The average  $z$  of the distribution increases as  $\epsilon_Q$  is reduced. It has been shown<sup>13</sup> that Eq. (1), with  $\epsilon_Q \simeq 0.25$ , is a satisfactory representation of measured charmed-meson momentum spectra.

We have fitted the contributions (i)–(iii) in

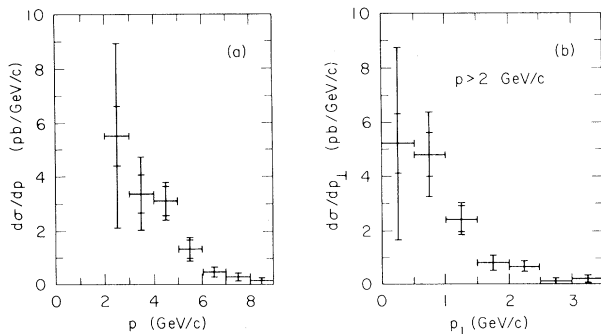


FIG. 2. Differential cross sections for prompt electrons with  $p > 2$  GeV/c: (a) total momentum and (b) transverse momentum.

terms of  $B_e(b)$  and  $B_e(c)$ , the average semielectronic branching ratios in  $b$ -quark and  $c$ -quark decay, and  $\epsilon_b$  and  $\epsilon_c$ , the parameters in Eq. (1) for  $b$  and  $c$  fragmentation. Average quark semielectronic branching ratios are equivalent to averages over all weakly decaying mesons and baryons, weighted by their relative populations. This point is particularly relevant to the charmed mesons with different  $B_e$  for  $D^+$  and  $D^0$ .<sup>6,14</sup> The total bottom and charm hadron populations are calculated from the number of observed events, under the assumption that quark pairs are produced in  $e^+e^-$  annihilation in proportion to the square of the quark charges. The interpretation of the parameters  $B_e(b)$  and  $B_e(c)$  as branching ratios depends on the validity of this assumption. We have also assumed that  $B_e(c)$  is the same for contributions (ii) and (iii), and that all bottom decays lead to charm.<sup>11,15</sup>

In the fit, we have fixed  $\epsilon_c$  at 0.25 in accordance with previous measurements of  $c$ -quark fragmentation.<sup>13</sup> For the remaining parameters we obtain  $B_e(b) = (11.6 \pm 2.1 \pm 1.7)\%$ ,  $B_e(c) = (6.3 \pm 1.2 \pm 2.1)\%$ , and  $\epsilon_b = 0.030^{+0.032}_{-0.018} {}^{+0.023}_{-0.014}$ . The quoted systematic errors reflect our estimates of uncertainties in the overall magnitude and momentum dependence of the hadron misidentification probabilities, the shape of the charm fragmentation function, the rest-frame momentum spectra of electrons from  $b$ - and  $c$ -quark decays, and the primordial  $p_\perp$  distributions of bottom and charm hadrons. The histograms in Fig. 1 show the results of the fit and the relative contributions of (i)–(iii) to the prompt electron signal in each  $p, p_\perp$  bin. The  $\chi^2$  per degree of freedom of the fit is 14.0/18, and the model that we have used gives a very good representation of the data over all  $p$  and  $p_\perp$  studied. We have verified that the value chosen for  $\epsilon_c$  is consistent with the data by performing an additional fit in which it was allowed to vary. The value obtained is compatible within errors with the input value of 0.25. Since we chose the parametrization in Eq. (1) *a priori*, we have not established the detailed shape of the fragmentation function, but only its peaking at large  $z$ . We have also studied a parametrization different from Eq. (1), namely of the form  $z^\alpha(1-z)$ , and obtain qualitatively similar results. For either of these parametrizations, the average value of  $z_b$  is  $\langle z \rangle_b = 0.75 \pm 0.05 \pm 0.04$ .

In conclusion, we have measured the total momentum and transverse momentum spectra for prompt electrons in hadronic events in  $e^+e^-$

annihilation at 29 GeV. We have extracted information on  $c$ - and  $b$ -quark semielectronic branching ratios and the  $b$ -quark fragmentation function based on a fit to these spectra. The values for the average semielectronic branching ratios,  $B_e(c) = (6.3 \pm 1.2 \pm 2.1)\%$  and  $B_e(b) = (11.6 \pm 2.1 \pm 1.7)\%$ , agree well with previous measurements<sup>6,10,11,14-16</sup> even though they may represent averages over slightly different hadron populations. The value of  $\epsilon_b$  and the corresponding average value of  $\langle z \rangle_b = 0.75 \pm 0.05 \pm 0.04$  strongly support the theoretical expectations of a bottom-quark fragmentation function which is peaked at large  $z$ .

This work was primarily supported by the Department of Energy under Contracts No. DE-AC03-76SF00515, No. DE-AC03-76SF00098, and No. DE-AC02-76ER03064.

---

<sup>(a)</sup>Present address: Laboratoire de Physique Nucléaires et Hautes Energies, Ecole Polytechnique, F-91128 Palaiseau, France.

<sup>(b)</sup>Present address: University of Arizona, Tucson, Ariz. 85721.

<sup>(c)</sup>Present address: Fermilab, Batavia, Ill. 60510.

<sup>(d)</sup>Present address: University of Massachusetts, Amherst, Mass. 01002.

<sup>1</sup>J. D. Bjorken, Phys. Rev. D 17, 171 (1978); M. Suzuki, Phys. Lett. 71B, 139 (1977).

<sup>2</sup>J. M. Yelton *et al.*, Phys. Rev. Lett. 49, 430 (1982).

<sup>3</sup>N. Abramowicz *et al.*, Z. Phys. C 15, 19 (1982).

<sup>4</sup>W. B. Atwood, Stanford Linear Accelerator Center Report No. SLAC-PUB-2980, 1982 (unpublished).

<sup>5</sup>M. J. Puhala *et al.*, Phys. Rev. D 25, 695 (1982).

<sup>6</sup>R. Schindler *et al.*, Phys. Rev. D 24, 78 (1981).

<sup>7</sup>G. S. Abrams, IEEE Trans. Nucl. Sci. 27, 59 (1980).

<sup>8</sup>R. D. Field and R. P. Feynman, Nucl. Phys. B136, 1 (1978).

<sup>9</sup>A. Ali *et al.*, Phys. Lett. 93B, 155 (1980).

<sup>10</sup>W. Bacino *et al.*, Phys. Rev. Lett. 43, 1073 (1979).

<sup>11</sup>K. Chadwick *et al.*, Cornell Laboratory of Nuclear Studies Report No. CLNS-82/546, 1982 (unpublished).

<sup>12</sup>C. Peterson *et al.*, Phys. Rev. D 27, 105 (1983).

<sup>13</sup>D. Schlatter, Stanford Linear Accelerator Center Report No. SLAC-PUB-2982, 1982 (unpublished).

<sup>14</sup>W. Bacino *et al.*, Phys. Rev. Lett. 45, 329 (1980).

<sup>15</sup>L. J. Spencer *et al.*, Phys. Rev. Lett. 47, 771 (1981).

<sup>16</sup>R. Brandelik *et al.*, Phys. Lett. 70B, 125, 387 (1977); J. M. Feller *et al.*, Phys. Rev. Lett. 40, 274, 1677 (1978).